THE UNIVERSITY *of* EDINBURGH

Edinburgh Research Explorer

Dipolar interactions, molecular flexibility, and flexoelectricity in bent-core liquid crystals

OPEN ACCESS

Dipolar interactions, molecular flexibility, and flexoelectricity in bent-core liquid crystals

Alastair Dewar and Philip J. Camp

Additional information on J. Chem. Phys.

Dipolar interactions, molecular flexibility, and flexoelectricity in bent-core liquid crystals

Alastair Dewar and Philip J. Camp[a)]
School of Chemistry, The University of Edinburgh, West Mains Road, Edinburgh EH9 3JJ,
United Kingdom

The effects of dipolar interactions and molecular flexibility on the structure and phase behavior of bent-core molecular fluids are studied using Monte Carlo computer simulations. Some calculations of flexoelectric coefficients are also reported. The rigid cores of the model molecules consist of either five or seven soft spheres arranged in a "V" shape with external bend angle γ. With purely repulsive sphere-sphere interactions and $\gamma=0°$ (linear molecules) the seven-sphere model exhibits isotropic, uniaxial nematic, and untilted and tilted smectic phases. With $\gamma \geqslant 20°$ the untilted smectic phases disappear, while the system with $\gamma \geqslant 40°$ shows a direct tilted smectic-isotropic fluid transition. The addition of electrostatic interactions between transverse dipole moments on the apical spheres is generally seen to reduce the degree of molecular inclination in tilted phases, and destabilizes the nematic and untilted smectic phases of linear molecules. The effects of adding three-segment flexible tails to the ends of five-sphere bent-core molecules are examined using configurational-bias Monte Carlo simulations. Only isotropic and smectic phases are observed. On the one hand, molecular flexibility gives rise to pronounced fluctuations in the smectic-layer structure, bringing the simulated system in better correspondence with real materials; on the other hand, the smectic phase shows almost no tilt. Lastly, the flexoelectric coefficients of various nematic phases—with and without attractive sphere-sphere interactions—are presented. The results are encouraging, but a large computational effort is required to evaluate the appropriate fluctuation relations reliably. © *2005 American Institute of Physics*. [DOI: 10.1063/1.2062007]

I. INTRODUCTION

There has been a surging interest in bent-core liquid crystals since their discovery in 1996.[1] Typically, these materials consist of molecules comprising rigid, banana-shaped cores made up of a conjugated system of linked aryl groups and flexible alkyl or alkoxy tails attached to each end. The molecules are usually achiral and possess electric dipole moments parallel with the molecular C_2 axis. One of the most intriguing properties of these compounds is that, in some cases, chiral ferroelectric or antiferroelectric smectic phases can be observed.[1–3] The chirality arises because the molecules tilt within the smectic layers; in chiral (anti)ferroelectric phases all of the molecules tilt in the same sense with respect to the layer polarization vector. It is not yet clear what is responsible for this spontaneous symmetry-breaking process, although a variety of explanations has been proposed. One popular explanation involves the long-range dipole-dipole interaction,[4] while recent theoretical work has identified a central role for dispersion interactions.[5] Other possible explanations include entropic "free-volume" mechanisms,[6] in which an antiferroelectric ordering of the smectic-layer polarizations affords more room for layer fluctuations, and mechanisms in which the molecules themselves spontaneously select chiral molecular conformations.[7]

There is a growing simulation literature on bent-core liquid crystals. One of the simplest bent-core molecular models

is a dimer made up of two hard spherocylinders.[6,8] This system exhibits isotropic, nematic, smectic, and crystalline phases, but no tilted phases. The Gay-Berne dimer model has been studied extensively, with and without molecular dipoles. In the works by Memmer[9] and Johnston *et al.*,[10,11] isotropic, nematic, tilted smectic, and helical phases were found, depending on the molecular bend angle[9,10] and the magnitude of the dipole moment.[11] Xu *et al.* studied composite molecules made up of repulsive soft spheres, and found isotropic and tilted crystalline phases.[12] More recently, we have studied composite molecules made up of the Lennard-Jones spheres—the so-called "composite Lennard-Jones molecules" (CLJMs)—which exhibit isotropic, nematic, tilted smectic, and tilted crystalline phases.[13]

In this work the effects of molecular dipole moments and molecular flexibility on the phase behavior of model bent-core molecules are studied using computer simulations. The model (to be detailed in Sec. II) consists of a rigid "V"-shaped core of soft spheres with a point dipole moment parallel to the C_2 axis. Molecular flexibility is included by the addition of short flexible tails to either end. There is a substantial literature on the effects of these molecular characteristics on linear molecules. In hard-spherocylinder fluids, the addition of longitudinal molecular dipoles is seen to destabilize the nematic phase, and can even destabilize smectic phases if the dipoles are displaced toward the ends of the molecules;[14,15] transverse dipoles also destabilize the nematic phase with respect to the smectic A.[16] Gay-Berne ellip-

a)Electronic mail: philip.camp@ed.ac.uk

soids with longitudinal point dipoles show a stabilization of the nematic phase with respect to the isotropic phase as the dipoles are moved from the centers of the molecules to the ends,[17] and can exhibit antiferroelectric smectic phases with striped structures.[18] Tilted polar smectic phases have been reported in fluids of Gay-Berne molecules with transverse dipole moments.[19] As far as molecular flexibility is concerned, the general consensus is that the introduction of flexible tail groups destabilizes the nematic phases of hard spherocylinders,[20] fused hard-sphere chains,[21,22] Gay-Berne,[23] and soft-sphere chains.[24] Interestingly, the simultaneous presence of flexible tails and molecular dipole moments can lead to a stabilization of the nematic phase.[25,26] With regard to bent-core molecules, Johnston *et al.* have shown that the presence of transverse molecular dipoles on Gay-Berne dimers stabilizes the smectic phases at the expense of nematic phases, increases the tilt angle in tilted smectic phases, and can induce long-range polar ordering.[11] In the current work we will show that for the bent-core soft-sphere models considered, the additions of dipolar interactions and flexible tails both destabilize the nematic phase, and that the dipolar interactions reduce the degree of molecular tilt in smectic phases.

This paper also reports our attempts to measure the flexoelectric coefficients[27,28] of model bent-core molecules. There are relatively few accounts of such measurements in literature. Experimentally, the determination of these quantities is highly nontrivial,[29,30] mainly due to the fact that the flexoelectric coefficients are not measured directly, but rather in linear combinations or as ratios involving elastic constants. In simulations, the flexoelectric coefficients of pear-shaped Gay-Berne ellipsoid/Lennard-Jones sphere molecules have been measured directly using expressions involving the direct correlation function.[31] The coefficients for a similar model were studied in simulations using fluctuation expressions.[32] The compound 5CB has been studied using a parametrized dipolar Gay-Berne model and the Percus-Yevick closure of the Ornstein-Zernike equation.[33,34] The flexoelectric coefficients were computed using the direct correlation function route, and the results compared moderately well with experiment.[29] A very recent simulation study of PCH5, using a fully atomistic molecular model, employed fluctuation formulas which yielded results in good agreement with experiment.[35] In the present work we critically assess the reliability of the fluctuation route in the context of our model systems, and show that the bend flexoelectric coefficients for nonpolar molecules can be comparable to those measured in experiments, reflecting the significant role of molecular packing in dense liquids.

This paper is organized as follows. In Sec. II the molecular model to be studied is fully defined, and the required simulation methods are described. The simulation results for rigid linear molecules are presented in Sec. III A, and those for rigid bent-core molecules in Secs. III B and III C. The effects of molecular flexibility are considered in Sec. III D, and flexoelectricity is discussed in Sec. III E. Section IV concludes the paper.
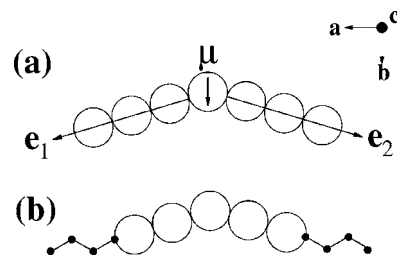

FIG. 1. The molecular models studied in this work: (a) the CSSM model and (b) the CSSMT model. Also shown are the molecular axes **a**, **b**, and **c**.

II. MOLECULAR MODEL AND SIMULATION METHODS

The molecular models considered in this work are shown schematically in Fig. 1. The most basic model [Fig. 1(a)] consists of a rigid core of seven soft spheres arranged in a V shape with external bond angle γ defined such that $\mathbf{e}_1 \cdot \mathbf{e}_2 = \cos(180° - \gamma)$, where $\mathbf{e}_1$ and $\mathbf{e}_2$ are unit vectors pointing along the two arms of the molecule. The sphere-sphere interaction potential is taken to be the repulsive part of the Lennard-Jones (12,6) potential, i.e.,

$$u_{ss}(r) = 4\epsilon \left(\frac{\sigma}{r} \right)^{12},$$ (1)

where r is the sphere-sphere separation, ϵ is an energy parameter, and σ is the sphere "diameter." The intramolecular sphere-sphere bond length is set equal to 1σ, and all short-range (soft sphere) potentials are truncated at 2.5σ. To identify the molecular axes that will be aligned in orientationally ordered phases, we define three unit vectors associated with the rigid cores of the molecules, as illustrated in Fig. 1. These vectors are given by $\mathbf{a} = (\mathbf{e}_1 - \mathbf{e}_2)/|\mathbf{e}_1 - \mathbf{e}_2|$, $\mathbf{b} = (\mathbf{e}_1 + \mathbf{e}_2)/|\mathbf{e}_1 + \mathbf{e}_2|$, and $\mathbf{c} = \mathbf{a} \wedge \mathbf{b}$.

Many real bent-core molecules possess a transverse electric dipole moment aligned along the C_2 molecular symmetry axis. To represent dipole-dipole interactions we have considered the model represented in Fig. 1(a), where a point dipole moment is placed at the center of the apical sphere along the C_2 symmetry axis (**b**). The dipole-dipole interaction is

$$u_{dd}(\mathbf{r}, \boldsymbol{\mu}_1, \boldsymbol{\mu}_2) = \frac{\boldsymbol{\mu}_1 \cdot \boldsymbol{\mu}_2}{r^3} - \frac{3(\boldsymbol{\mu}_1 \cdot \mathbf{r})(\boldsymbol{\mu}_2 \cdot \mathbf{r})}{r^5},$$ (2)

where $\mathbf{r}$ is the pair separation vector, $r = |\mathbf{r}|$, and $\boldsymbol{\mu}_i = \mu \mathbf{b}_i$ is the dipole vector on particle i. For brevity, we shall refer to these molecules as "composite soft-sphere molecules" (CSSMs).

Common additional features of real bent-core molecules include alkyl or alkoxy chains (typically 3–12 carbons in length) attached to both ends of each molecule. To represent these tails we consider the addition of four extra spheres at each end of the model molecules, as represented in Fig. 1(b). The first sphere in each tail (nearest the core) is fixed in line with the arm at a distance of 0.5σ from the center of the terminal core sphere. All subsequent tail segments are allowed to pivot freely (with no torsional potential) under the following constraints: The tail bond lengths are equal to 0.6σ, which corresponds to the ratio of the carbon-carbon bond length to the diameter of the aromatic ring in real bent-core liquid crystals; each tail segment is oriented at the tet-

rahedral angle, $\cos^{-1}(-\frac{1}{3}) = 109.47°$, with respect to its neighboring segments, mimicking the bond angles in a simple hydrocarbon tail. Clearly this extension will cause a considerable increase in the number of interactions to be evaluated, so to make the simulations tractable we have made the following simplifications. Firstly, we have reduced the size of the rigid bent core to five spheres. (With the addition of the tail segments, this actually makes the effective elongations for all of the models considered to be more comparable.) Secondly, we neglect interactions between tails on different molecules. Within the Lorentz-Berthelot mixing rules,[36] this corresponds to setting the tail-sphere diameter to zero. Denoting the core and tail spheres by "c" and "t," respectively, the interaction potential is

$$u_{ss}^{ij}(r) = 4\epsilon\left(\frac{\sigma_{ij}}{r}\right)^{12},\tag{3}$$

with $i, j = c$ or t, $\sigma_{cc} = \sigma$, $\sigma_{tt} = 0$, and $\sigma_{ct} = \frac{1}{2}(\sigma_{cc} + \sigma_{tt}) = \frac{1}{2}\sigma$, and for simplicity the energy parameter ϵ is the same for all pairs. This is clearly a very crude representation of molecular flexibility, but it has proven to be an appropriate means of extending the range of applicability of simple liquid-crystal models.[20,25] Even though this is a simple model, configurational-bias Monte Carlo (MC) techniques are required to simulate the system efficiently; these are summarized in Sec. II A. For brevity, we shall refer to these molecules as "composite soft-sphere molecules with tails" (CSSMTs).

Reduced units for these systems are defined as follows: reduced molecular density $\rho^* = N_m\sigma^3/V$, where N_m is the number of molecules and V is the system volume, reduced temperature $T^* = k_BT/\epsilon$, reduced pressure $p^* = p\sigma^3/\epsilon$, and reduced dipole moment $\mu^* = \sqrt{\mu^2/\epsilon\sigma^3}$.

A. Monte Carlo

The phase behavior of the model systems was investigated using constant-pressure (N-P-T) and constant-volume (N-V-T) Metropolis MC simulations.[36] In all of the simulations reported in this work the number of molecules was $N_m = 400$, with initial high-density crystalline configurations consisting of four layers of 100 molecules. The general approach was to equilibrate the system at low temperature ($T^* \sim 1$) and high density ($\rho^* \sim 0.14$) using N-V-T simulations in a cuboidal simulation cell with dimensions $L_x = L_y \neq L_z$ and volume $V = L_xL_yL_z$, and then switching over to N-P-T simulations in which $L_x = L_y$ and L_z were sampled independently, thus allowing the box to change shape. As explained in Ref. 13, spotchecks on the stress tensor showed that the cuboidal/cubic cells did not mechanically destabilize liquid-crystalline phases. Our earlier work indicated that all of the expected liquid-crystalline phases could be stabilized in a CLJM system at a pressure of $p^* = 4$, and so we used this value throughout. Simulations along the isobar were carried out at progressively higher temperatures in order to locate phase transitions between solid, smectic, nematic, and isotropic phases. Transitions were identified by measuring the equation of state (density as a function of temperature), relevant orientational order parameters, and radial distribution

functions (detailed below). Cooling runs were carried out using cuboidal and/or cubic simulation cells to confirm the existence and nature of the transitions.

For the CSSM system, straightforward simulation techniques were employed as detailed in our earlier work;[13] single-particle translation and rotation moves and volume moves (in $\ln V$ or $\ln L$) were generated with respective maximum displacement parameters to achieve $\sim 50\%$ acceptance rates. The long-range dipolar interactions were handled using Ewald summations with conducting ("tin foil") boundary conditions.[36]

For the CSSMT system the configurational-bias MC (CBMC) technique was implemented and optimized as described in Refs. 37 and 38. Tail conformations were sampled by generating five trial orientations per segment per MC move. Translational and rotational displacement parameters were adjusted to give an acceptance ratio of 10%; in N-P-T simulations the volume moves were adjusted to give a 50% acceptance ratio. The computational effort required to simulate this system was considerable. Carrying out a MC sweep consisting of one attempted translation and rotation per molecule and one volume move took approximately 4 s on a 2.2 GHz Intel Xeon processor; achieving, equilibration at each state point required at least 10^5 MC sweeps.

To monitor orientational order, the order tensors $\mathbf{Q}_{\alpha\alpha} = \frac{1}{2}\Sigma_{i=1}^{N}(3\boldsymbol{\alpha\alpha} - 1)$ for each of the molecular axes $\boldsymbol{\alpha} = \mathbf{a}$, $\mathbf{b}$, and $\mathbf{c}$ were diagonalized yielding the eigenvalues $\lambda_\alpha^- < \lambda_\alpha^0 < \lambda_\alpha^+$ and the corresponding orthonormal eigenvectors $\mathbf{n}_\alpha^-$, $\mathbf{n}_\alpha^0$, and $\mathbf{n}_\alpha^+$.[39] The molecular x, y, and z axes were then assigned in order of increasing λ_α^+, and the laboratory axes $\mathbf{X}$, $\mathbf{Y}$, and $\mathbf{Z}$ were identified with the corresponding directors. In practice this invariably meant that the molecular z axis was the "long" axis $\mathbf{a}$ and the x and y axes were $\mathbf{b}$ and $\mathbf{c}$, and that the laboratory z axis was $\mathbf{n}_a^+$. The usual nematic and biaxial order parameters, S and Q_{22}^2, are then given by

$$S = \mathbf{Z} \cdot \mathbf{Q}_{zz} \cdot \mathbf{Z},\tag{4}$$

$$Q_{22}^2 = \frac{1}{3}(\mathbf{X} \cdot \mathbf{Q}_{xx} \cdot \mathbf{X} + \mathbf{Y} \cdot \mathbf{Q}_{yy} \cdot \mathbf{Y} - \mathbf{X} \cdot \mathbf{Q}_{yy} \cdot \mathbf{Y} - \mathbf{Y} \cdot \mathbf{Q}_{xx} \cdot \mathbf{Y}).\tag{5}$$

In a perfect uniaxial nematic phase, $S = 1$ and $Q_{22}^2 = 0$, whereas in a perfect biaxial phase, $S = 1$ and $Q_{22}^2 = 1$. In practice no biaxial ordering was detected in any of the simulations, and so we will not report the numerical values of Q_{22}^2 (which are less than ~ 0.1).

To help characterize smectic phases, the correlations between molecules in the same smectic layer were examined using an in-layer (two-dimensional) radial distribution function $g_{xy}(r)$ defined by

$$g_{xy}(r) = \left\langle \frac{L_xL_y}{2\pi r N_1^2}\sum_{i=1}^{N_1}\sum_{j\neq i}^{N_1}\delta(|\mathbf{r}_i - \mathbf{r}_j| - r)\right\rangle,\tag{6}$$

where N_1 is the number of molecules within the layer, and $\mathbf{r}_i$ is the position vector of the apical sphere on the ith molecule.

Some additional measured observables include the polarization $\mathbf{P} = \mu\Sigma_i\mathbf{b}_i$ and the intermolecular torque-density ten-
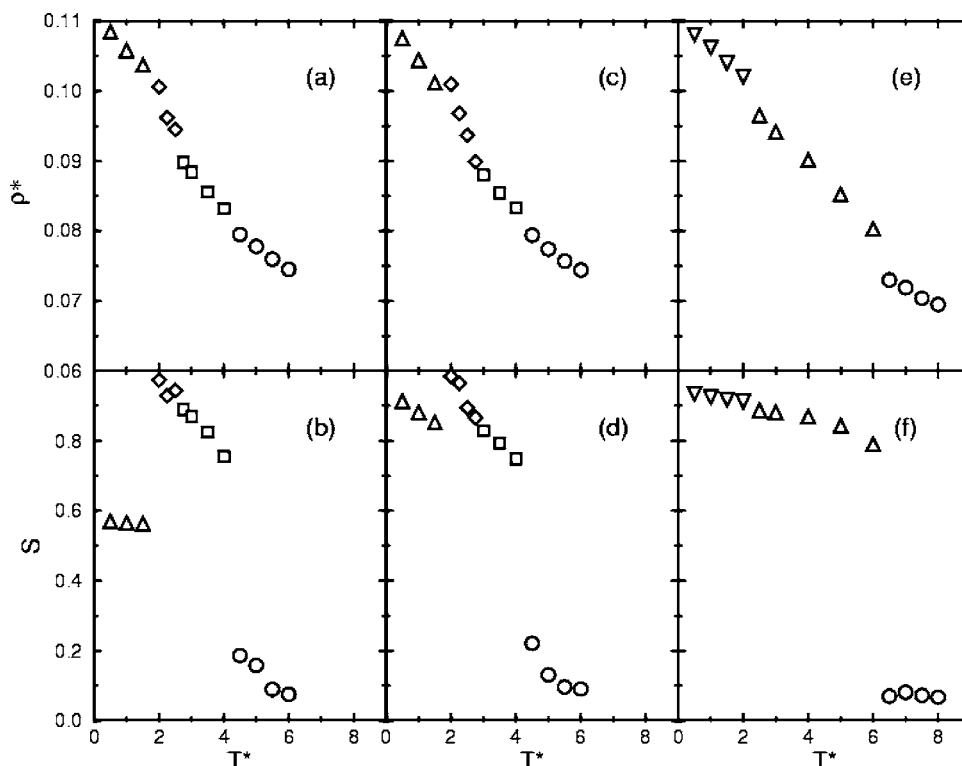
FIG. 2. Equations of state [(a),(c),(e)] and order parameters [(b),(d),(f)] for CSSM systems with $\gamma=0°$ along an isobar with $p^*=4$: [(a),(b)] $\mu^*=0$, [(c),(d)] $\mu^*=1$, and [(e),(f)] $\mu^*=2$. The symbols denote different phases: solid (down triangles), tilted smectic F (up triangles), untilted smectics (diamonds), nematic (squares), and isotropic (circles).

sor $\mathbf{\Pi}$. In particular, these quantities are required for the calculation of flexoelectric coefficients, full details of which will be given in Sec. III E.

III. RESULTS

In what follows we use standard designations for untilted and tilted smectic phases:[40,41] smectic A for untilted phases with fluid in-layer order, smectic B for untilted phases with hexatic or crystalline in-layer order, smectic C for tilted phases with fluid in-layer order, and smectic F for tilted phases with hexatic in-layer order.

A. CSSMs with $\gamma=0°$

The equation of state and order parameters for apolar ($\mu^*=0$) linear CSSMs along an isobar with $p^*=4$ are shown in Figs. 2(a) and 2(b), respectively. In order of increasing temperature we find a high-density tilted phase ($0.5 \leqslant T^*$

$\leqslant 1.5$), untilted smectics ($2 \leqslant T^* \leqslant 2.5$), a uniaxial nematic ($2.75 \leqslant T^* \leqslant 4$), and ultimately the isotropic phase ($T^* \geqslant 4.5$). Simulation snapshots are shown in Fig. 3.

In the tilted phase, the molecules are arranged in layers tilted by about 60° with respect to each other, as shown in Fig. 3(a). This "herringbone" structure clearly allows close packing of the constituent spheres. It is difficult to resolve the molecules in to layers by eye, but it is quite clear from examining simulation snapshots that there is no long-range crystalline order. The in-layer radial distribution function $g_{xy}(r)$ should have provided some insights on the nature of this phase; the results for the appropriate temperature range ($0.5 \leqslant T^* \leqslant 1.5$) are shown in Fig. 4. It is not at all clear what type of ordering is present, so in the absence of any firm evidence we tentatively assign this phase as smectic F since we know that it is tilted and that it does not show any long-range crystalline order.

The tilted-untilted smectic transition is clearly accompa-
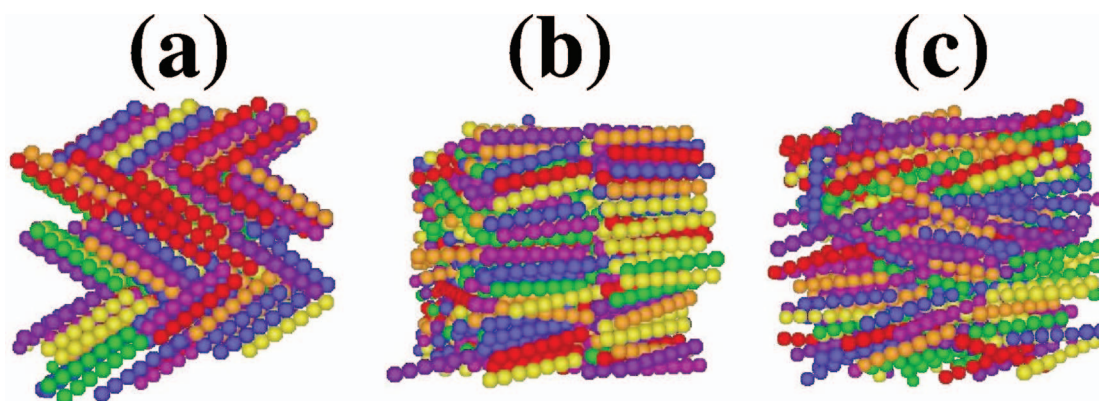

FIG. 3. (Color) Simulation snapshots of the CSSM system with $\gamma=0°$ (linear molecules) along an isobar with $p^*=4$: (a) tilted smectic F ($\mu^*=0$, $T^*=2$), (b) smectic A ($\mu^*=0$, $T^*=2.5$), and (c) nematic ($\mu^*=0$, $T^*=4$).
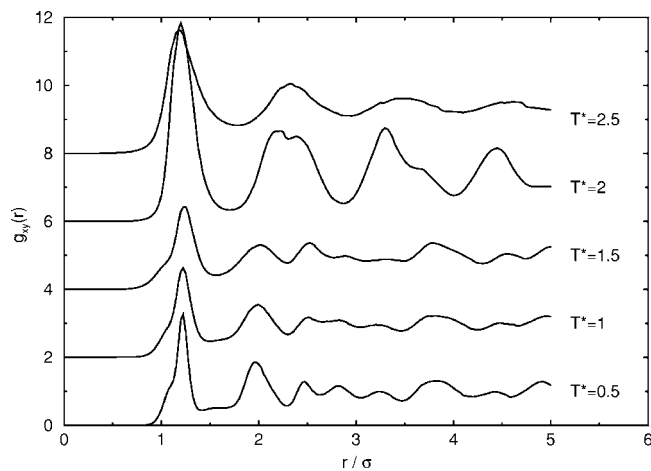
FIG. 4. In-layer radial distribution functions $g_{xy}(r)$ for the CSSM system with $\gamma=0°$ (linear molecules) and $\mu^*=0$ along an isobar with $p^*=4$ and at different temperatures. The curves are displaced by 2 u along the ordinate for clarity.

nied by a significant change in the intralayer structure; $g_{xy}(r)$ in the temperature range of $0.5 \leqslant T^* \leqslant 2.5$ is shown in Fig. 4, and simulation snapshots are shown in Fig. 3. The results for $T^*=2$ and $T^*=2.5$ suggest that there is a smectic B–smectic A transition in this system; at the lower temperature the split second peak is a characteristic of hexatic order. In the equation of state [Fig. 2(a)] there is the slightest indication of a transition between $T^*=2$ and $T^*=2.25$, but it is difficult to make any definitive statements on these results alone.

Referring to Fig. 2(b), the jump in the nematic order parameter in the temperature range of $1.5 < T^* < 2$ is due to the transition from the tilted smectic F phase to an untilted smectic B phase; the drop in the range of $4 < T^* < 4.5$ signals the nematic-isotropic transition. In all, the results for this system are in good qualitative correspondence with those for a whole host of similar (linear) molecular models, including soft-sphere chains[42] and the Lennard-Jones chains.[43] The results are also comparable to those presented in Ref. 13 for seven-sphere CLJM fluids in which the sphere-sphere interaction is given by $4\epsilon[(\sigma/r)^{12}-(\sigma/r)^6]$. Qualitatively, the CSSM and CLJM systems are very similar, but in the latter case the phase transitions are shifted to higher temperatures due to the attractive component of the interaction potential.

The same process of phase identification was applied to simulated polar systems. With the addition of a small molecular dipole ($\mu^*=1$) we see little qualitative difference in the equation of state at $p^*=4$, as shown in Fig. 2(c). Despite the small change in the equation of state, the gross structure of the tilted smectic F phase is quite different from that in the apolar system. The low-temperature smectic F phase is not so strongly tilted as in the apolar system, exhibiting a tilt angle with respect to the layer normal of $\sim 20°$. This is most likely to allow dipoles on neighboring molecules to attain the low-energy "nose-to-tail" conformation within the plane of the layer. The nematic order parameter—shown in Fig. 2(d)—is relatively high at temperatures $T^* \leqslant 1.5$ due to the reduced degree of tilt. The smectic F–smectic A and smectic A–nematic transitions give rise to the abrupt changes in S at $1.5 < T^* < 2$ and $4 < T^* < 4.5$, respectively.

With a large dipole moment ($\mu^*=2$) and $p^*=4$ we see some dramatic differences in the phase behavior: Nematic and untilted smectic phases are completely absent, and there is instead a distinct transition between two high-density layered phases in the range of $2 \leqslant T^* \leqslant 2.5$. The simulation snapshots at temperatures of $T^*=2$ and $T^*=4$ are shown in Fig. 5. Figures 5(c) and 5(d) show that at $T^* \leqslant 2$ the system is in a crystalline phase, with apparently long-range positional order within the layers. At $T^*=4$ the in-layer ordering is qualitatively different, showing short-range positional correlations and defects that destroy long-range positional order; $g_{xy}(r)$ at this temperature is very similar to that for the apolar system at $T^*=2$ (Fig. 4). The equation of state and nematic order parameter are shown in Figs. 2(e) and 2(f). We assign the branches in the equation of state as corresponding to crystalline ($0.5 \leqslant T^* \leqslant 2$), tilted smectic F ($2.5 \leqslant T^* \leqslant 6$), and isotropic ($T^* \geqslant 6.5$) phases.

To summarize, the addition of dipolar interactions to linear seven-sphere molecules leads to a reduction in the degree of tilt in the low-temperature smectic F phase. With high dipole moments, the untilted smectic and nematic phases disappear, and a solid-smectic F transition is shifted in to the range of temperatures considered in this work.

B. CSSMs with $\gamma=20°$

The equations of state and nematic order parameters for CSSM systems with $\gamma=20°$ along an isobar with $p^*=4$ are shown in Fig. 6. Results are shown for two dipole moments, $\mu^*=0$ [Figs. 6(a) and 6(b)] and $\mu^*=1$ [Figs. 6(c) and 6(d)]. Both the apolar and polar systems exhibit tilted smectic F, nematic, and isotropic phases; examples of the smectic and nematic phases in the $\mu^*=0$ system are illustrated in Fig. 7. In the smectic F phases it was observed that the degree of molecular tilt with respect to the layer normal is far greater in the apolar case ($\sim 53°$) than in the polar case ($< 20°$). The smectic F–nematic phase transition appears to be more pronounced in the apolar system than in the polar system, as evidenced by the associated features in the equations of state and in the variations of the nematic order parameters. Some simulations were attempted with $\mu^*=2$ but these suffered from convergence problems; simulations with different initial configurations failed to converge on to the same branch of the equation of state. It is possible that this was due to the combination of the steric dipole (molecular bend) and the "electric" dipole resulting in strong anisotropic interactions and prohibitively slow convergence.

A comparison of Figs. 2 and 6 shows that the presence of a modest molecular bend leads to the untilted smectic phases being destabilized. This same trend was observed in the simulations of the CLJM system.[13] The introduction of dipolar interactions to the bent-core model then seems to stabilize the nematic phase slightly in favor of the smectic F. The smectic F phases themselves are tilted, but the degree of tilt is reduced significantly upon the addition of dipolar interactions. This perhaps provides a clue as to why dipolar interactions apparently disfavor the smectic F; the bent cores want to form a tilted phase, but the dipolar interactions want an untilted phase as explained in Sec. III A.
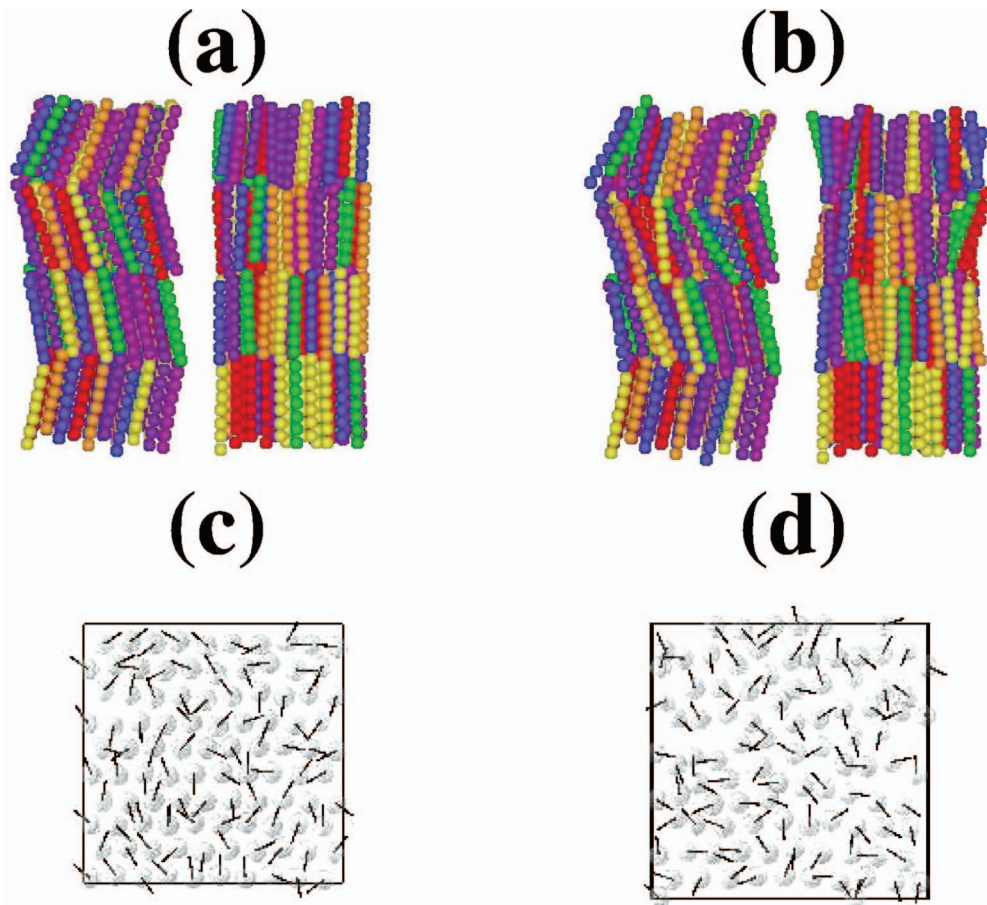
FIG. 5. (Color) Simulation snapshots of the CSSM system with $\gamma=0°$ and $\mu^*=2$: (a) crystalline phase ($T^*=2$), (b) tilted smectic F phase ($T^*=4$), (c) a typical layer in the crystalline phase ($T^*=2$), and a typical layer in the tilted smectic F phase ($T^*=4$). In (c) and (d) the short black lines indicate the orientations of the molecular dipole moments.
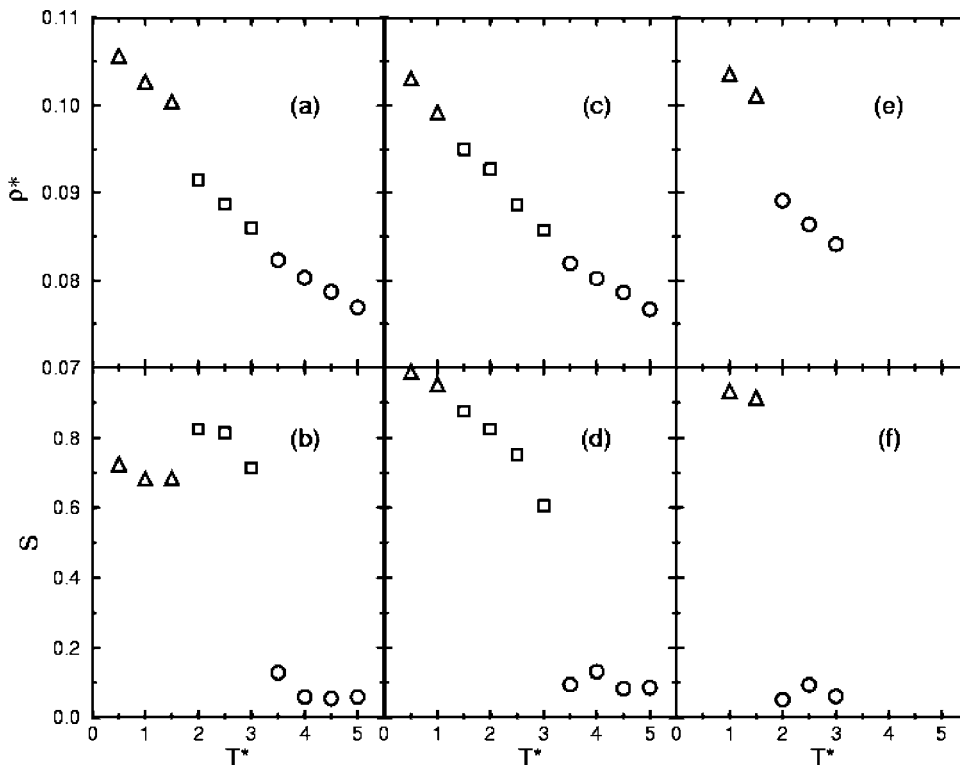

FIG. 6. Equations of state [(a),(c),(e)] and order parameters [(b),(d),(f)] for CSSM systems with $\gamma=20°$ and $\gamma=40°$ along an isobar with $p^*=4$: [(a),(b)] $\gamma=20°$ and $\mu^*=0$, [(c),(d)] $\gamma=20°$ and $\mu^*=1$, and [(e),(f)] $\gamma=40°$ and $\mu^*=0$. The symbols denote different phases: tilted smectic F (up triangles), nematic (squares), and isotropic (circles).
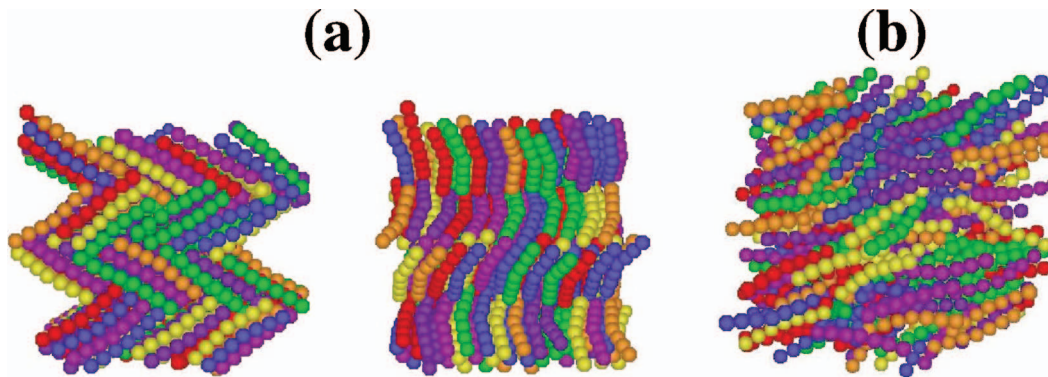
FIG. 7. (Color) Simulation snapshots of the CSSM system with $\gamma=20°$ along an isobar with $p^*=4$: (a) two views of the tilted smectic F at $T^*=1$ and (b) nematic phase at $T^*=3$.

C. CSSMs with $\gamma=40°$

The convergence problems encountered with the $\gamma=20°$ system were exacerbated by an increase of the bend angle to $\gamma=40°$. In this case it was only possible to achieve reliable results for the apolar system. The results at $\mu^*=0$ and $p^*=4$ are shown in Figs. 6(e) and 6(f). The equation of state and order parameters show only two branches, which correspond to tilted smectic F and isotropic phases. This is very similar to the situation in the CLJM system with the same bend angle,[13] albeit with the CSSM system undergoing a phase transition at lower temperature.

D. CSSMTs

We performed N-P-T simulations of CSSMT systems with bend angles of $\gamma=0°$, 20°, and 40° along an isobar with $p^*=4$. Due to the computational effort required for these simulations we were not able to map out equations of state as comprehensive as those for the CSSM systems. The simulation results are presented in Table I. The only phases observed in our simulations were smectic and isotropic. In all cases the smectics were stable at $T^*\leqslant 1.5$, and the smectic-isotropic transition occurred in the range of $1.5\leqslant T^*\leqslant 2$. Some simulation snapshots of the smectic phases are shown

in Fig. 8. In all cases the translational ordering within the layers was of the smectic-B-type, i.e., local hexagonal coordination. The systems with $\gamma=0°$ and $\gamma=20°$ showed no appreciable molecular tilt within the smectic layers, while the $\gamma=40°$ system showed an unusual "grain-boundary" structure between the clearly demarcated domains of the untilted smectic. Larger-scale simulations will be required to determine whether this is a signal of a long-wavelength-modulated structure. Given these observations, we assign the layered phases as smectic B. It is particularly striking that the smectic-layer fluctuations are much larger than those in the CSSM [and CLJM (Ref. 13)] systems. Indeed, one criticism of the latter models—and other rigid-rod models—is that the smectics are too well ordered. Unsurprisingly, the introduction of molecular flexibility has improved the correspondence between simulated smectic structures and those inferred from light-scattering experiments on common (flexible or semiflexible) mesogens.[28]

The conformations of the flexible tail groups were investigated using some simple measures. The extension of each tail was identified with the distance l, between the first and fourth joints (the black spheres in Fig. 1). The probability

TABLE I. Results from N-P-T simulations of the CSSMT system along an isobar with $p^*=4$. The digits in parentheses denote the estimated statistical uncertainty in the last figure.

| γ/degrees	T^*	ρ^*	S	l/σ	γ_{eff}/degrees
0	1	0.1098(4)	0.918	5.48(1)	48.0(3)
0	1.5	0.1018(4)	0.725	5.82(1)	29.6(2)
0	2	0.1067(7)	0.091	5.40(3)	31.8(3)
0	2.5	0.1019(7)	0.097	5.45(3)	32.3(3)
0	3	0.0981(7)	0.063	5.44(2)	32.5(3)
20	1	0.1128(2)	0.865	5.41(1)	50.9(4)
20	1.5	0.1101(2)	0.787	5.51(1)	43.3(2)
20	2	0.1057(7)	0.200	5.35(3)	37.0(5)
20	2.5	0.1010(3)	0.062	5.34(3)	37.4(4)
20	3	0.0976(7)	0.054	5.34(2)	37.6(4)
40	1	0.1161(3)	0.879	4.98(1)	65.2(4)
40	1.5	0.1084(1)	0.833	4.93(1)	60.7(2)
40	2	0.1048(6)	0.067	5.08(3)	49.5(3)
40	2.5	0.1008(6)	0.081	5.10(2)	49.2(6)
40	3	0.0974(7)	0.057	5.11(2)	49.4(5)
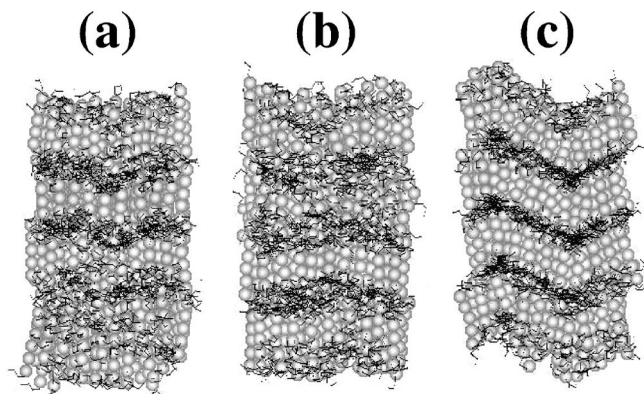
FIG. 8. Simulation snapshots of CSSMT systems at $T^*=1$ and $p^*=4$: (a) $\gamma=0°$, (b) $\gamma=20°$, and (c) $\gamma=40°$.

density function $p(l)$ is shown in Fig. 9 for all of the CSSMT systems at $T^*=1$ (smectic B) and $T^*=3$ (isotropic). Each function shows peaks at $l/\sigma=1$ and $l/\sigma\simeq1.5$. For a perfect *cis* conformation the tail extension is 5/3 times the bond length, while for the *trans* conformation it is $\sqrt{19/3}$ times the bond length. With the bond length being 0.6σ, these distances correspond to $l/\sigma=1$ and $l/\sigma\simeq1.51$, respectively. Firstly, the *cis* conformation is clearly the more favorable, presumably because the molecules strive to attain the shortest effective elongation to minimize excluded-volume interactions. Interestingly, for each system the *cis* conformation appears slightly more favorable in the isotropic phase than in the smectic phase. This may be due to the opportunity for interdigitation of the tails with the cores in neighboring smectic layers, which would explain the accompanying increase in the occurrence of the *trans* conformation.
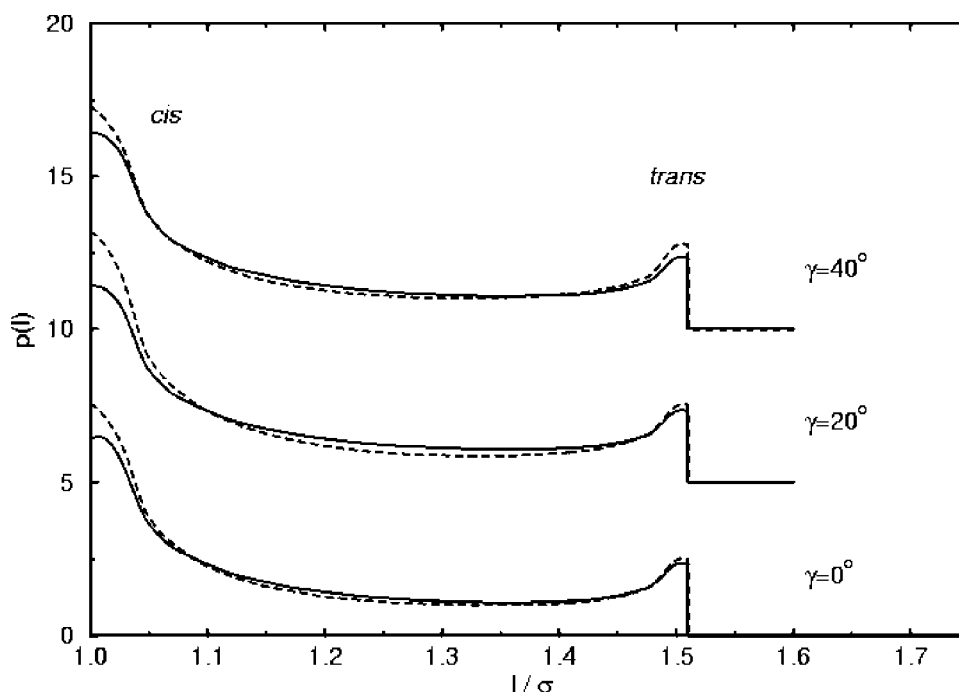
The effective molecular bend angle was determined by calculating the dot product of the two unit vectors linking the apical sphere to the terminal tail units, $\mathbf{u}_1$ and $\mathbf{u}_2$; the required angle is then $\gamma_{\text{eff}}=\cos^{-1}(-\mathbf{u}_1\cdot\mathbf{u}_2)$. The values of γ_{eff} are reported in Table I. For each system $\gamma_{\text{eff}}>\gamma$ which shows that the tails must curl up in such a way as to make the molecule more banana shaped. In the smectic phases this can be observed directly in Fig. 8, where the tails prefer to be oriented in the plane of the smectic layers, rather than pointing straight down toward the neighboring layers. This idea is confirmed by the fact that the effective molecular bend is more pronounced in the smectic phase than in the isotropic phase.

In summary, the addition of molecular flexibility results in the disappearance of the nematic phase, and in the case of the linear molecules the smectic A phase as well. This is in good qualitative agreement with the trends observed in a variety of other liquid-crystal models.[20–24,26] The smectic-layer structures of the flexible model systems correspond more closely to those in real smectic liquid crystals.

E. Flexoelectric coefficients

In 1969 Meyer predicted the existence of what is now known as the *flexoelectric effect* in nematic liquid crystals, in which the long-wavelength distortions of the local molecular alignment (director field **n**) give rise to a bulk polarization **P**.[27] The textbook explanation of the effect is that if the director field possesses curvature then an asymmetric molecular shape can dictate a favorable local packing arrangement which, in the presence of molecular dipoles, may give rise to a polarization.[28] With a splay deformation ($\nabla\cdot\mathbf{n}\neq0$) wedge-

FIG. 9. Tail-length distribution functions for the terminal four-center tails in CSSMT systems along an isobar with $p^*=4$: (bottom) $\gamma=0°$, (middle) $\gamma=20°$, and (top) $\gamma=40°$. The curves for each bond angle are displaced by 10 u along the ordinate for clarity. In each case the solid lines correspond to $T^*=1$ and the dashed lines to $T^*=3$. With bond lengths of 0.6σ the pure *cis* conformation corresponds to $l=(5/3)\times0.6\sigma=\sigma$, and the pure *trans* conformation to $l=\sqrt{19/3}\times0.6\sigma\simeq1.51\sigma$.
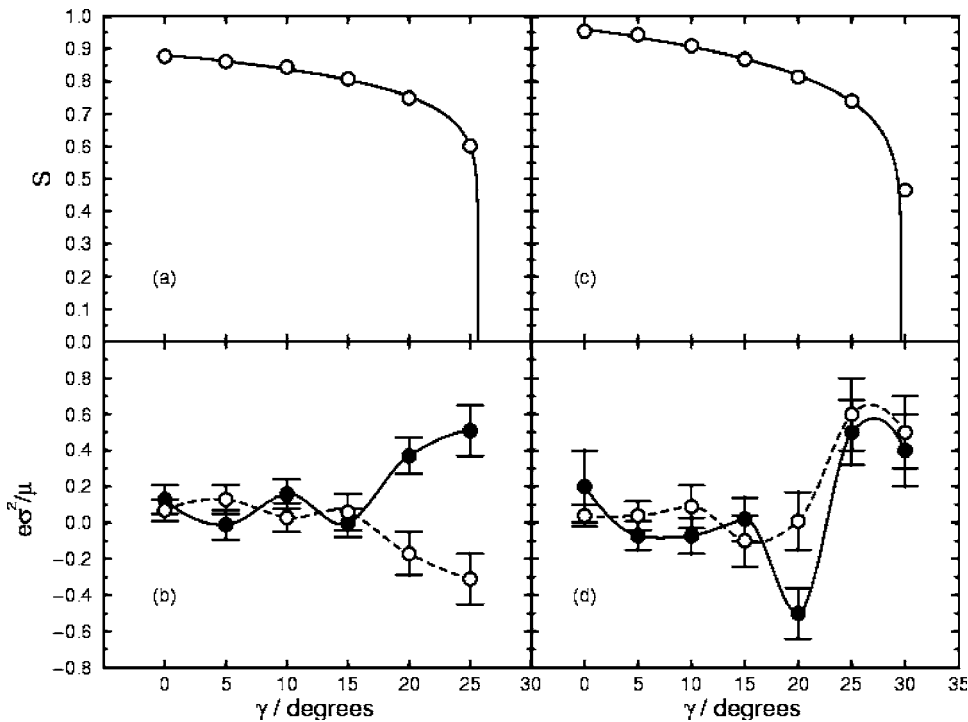
FIG. 10. Nematic order parameters [(a),(c)] and flexoelectric coefficients [(b),(d)] for the CSSM system at $\rho^*=0.0888$ and $T^*=3$ [(a),(b)] and the CLJM system at $\rho^*=0.1155$ and $T^*=6.5$ [(c),(d)]. In (b) and (d) the flexoelectric coefficients are those corresponding to splay deformations (filled symbols) and bend deformations (open symbols). The lines are spline fits to guide the eye.

shaped molecules with longitudinal dipole moments pack most efficiently when the dipoles are aligned. With a bend deformation $(|\nabla \wedge \mathbf{n}| \neq 0)$ banana-shaped molecules with transverse dipole moments are arranged preferentially to give a net polarization. General symmetry arguments lead to the following relationship between the polarization density $\mathbf{p} = V^{-1}\mathbf{P}$ (units of C m^{-2}) and the lowest order deformations of the director field:

$$\mathbf{p} = e_1(\nabla \cdot \mathbf{n})\mathbf{n} + e_3(\nabla \wedge \mathbf{n}) \wedge \mathbf{n}, \qquad (7)$$

where e_1 and e_3 are the splay and bend flexoelectric coefficients, respectively, with units of C m^{-1}. Historically there is some ambiguity in the sign of e_3; to be clear, throughout this work we employ the convention used by Meyer in his original study,[27] Nemtsov and Osipov in their analysis of flexoelectricity in the context of linear-response theory,[44] and de Gennes and Prost in their canonical text.[28] Allen and Masters have supplied a comprehensive account of various simulation methods for measuring the flexoelectric coefficients.[45] Following the sign conventions in Ref. 45 we have calculated e_1 and e_3 using the following relationships:

$$e_1 = \frac{1}{2}\beta V^{-1}(\langle P_z\Pi_{xy}\rangle - \langle P_z\Pi_{yx}\rangle), \qquad (8)$$

$$e_3 = \frac{1}{2}\beta V^{-1}(\langle P_y\Pi_{zx}\rangle - \langle P_x\Pi_{zy}\rangle), \qquad (9)$$

where $\mathbf{\Pi} = -\Sigma_{i<j}\mathbf{r}_{ij}\boldsymbol{\tau}_{ij}$ is the orientational stress density tensor, $\mathbf{r}_{ij} = \mathbf{r}_i - \mathbf{r}_j$ is the intermolecular separation vector, and $\boldsymbol{\tau}_{ij}$ is the torque on molecule i due to molecule j. $\boldsymbol{\tau}_{ij}$ was calculated as a sum of moments of the sphere-sphere interactions about the apical sphere, and all vectors and tensors were calculated in a frame in which the laboratory z axis coincides with the nematic director $\mathbf{n}_a^+$. It is easy to show that the combinations $P_z\Pi_{xy} - P_z\Pi_{yx}$ and $P_y\Pi_{zx} - P_x\Pi_{zy}$ are invariant

with respect to a rotation of the x and y axes about $\mathbf{n}$, and so the assignments of the x and y axes are arbitrary. It should be noted that we only have calculated the flexoelectric coefficients for nonpolar systems. The "steric dipole" is still parallel to $\mathbf{b}$ in Fig. 1, but there are no *electrostatic* dipole-dipole interactions. The polarization is given by $\mathbf{P} = \mu\Sigma_{i=1}^{N_m}\mathbf{b}_i$, and carries the trivial factor of μ by virtue of there being no electrostatic interactions.

The flexoelectric coefficients have been calculated in the nematic phases of nonpolar CSSM and CLJM (Ref. 13) systems as a function of the molecular bend angle γ. For the purposes of comparison, the CSSM system has been studied at a fixed density and temperature for which the nematic phase is stable at several values of γ. An examination of Figs. 2(a) and 6(a) shows that in the range of $0° \leq \gamma \leq 20°$, the nematic phase is stable at temperatures and densities in the regions of $T^* \sim 3$ and $\rho^* \sim 0.085$, respectively. A particular state point from the $\gamma = 0°$ system was selected arbitrarily for all of the simulations, this being $T^* = 3$ and $\rho^* = 0.0888$. Canonical $(N\text{-}V\text{-}T)$ simulations were used to equilibrate nematic phases for systems with bend angles in the range of $0° \leq \gamma \leq 25°$. The nematic order parameter S is shown as a function of γ in Fig. 10(a). We found that S could be fitted with a power law,

$$S(\gamma) = S(0)\left(1 - \frac{\gamma}{\gamma_c}\right)^\alpha, \qquad (10)$$

where $S(0)$ is the order parameter for linear molecules, γ_c is a critical bend angle above which the nematic phase is no longer thermodynamically stable, and α is a specific exponent. The fit is shown in Fig. 10(a); the fit parameters were $S(0) = 0.881(4)$, $\gamma_c = 25.6(2)°$, and $\alpha = 0.104(7)$. A similar procedure was carried out for the CLJM system studied in Ref. 13. Nematic phases were simulated at $T^* = 6.5$ and $\rho^* = 0.1155$ for systems with $0° \leq \gamma \leq 30°$. The nematic order

TABLE II. Results from N-V-T simulations of CSSM and CLJM systems in the nematic phase at reduced density ρ^* and reduced temperature T^*. γ is the molecular bend angle, S is the nematic order parameter, $e_1^* = e_1\sigma^2/\mu$ and $e_3^* = \sigma^2/\mu$ are the reduced splay and bend flexoelectric coefficients, respectively, and P_α is the average of the α component of the system polarization. The digits in parentheses denote the estimated statistical uncertainty in the last figure based on two standard deviations.

γ/degrees	S	e_1^*	e_3^*	P_x/μ	P_y/μ	P_z/μ
		CSSM, $T^*=3$, $\rho^*=0.0888$				
0	0.877	0.13(4)	0.07(3)	−0.21(4)	0.77(6)	1.43(2)
5	0.861	−0.01(4)	0.13(4)	−0.31(6)	−0.38(6)	0.02(2)
10	0.844	0.16(4)	0.03(4)	0.27(6)	−0.38(6)	−0.10(2)
15	0.807	−0.00(4)	0.06(5)	0.90(6)	−1.04(6)	0.56(2)
20	0.749	0.37(5)	−0.17(6)	0.09(6)	−0.55(6)	0.67(4)
25	0.601	0.51(7)	−0.31(7)	−1.10(6)	1.00(6)	−0.75(4)
		CLJM, $T^*=6.5$, $\rho^*=0.1155$				
0	0.954	0.2(1)	0.04(3)	−0.13(6)	−0.78(6)	−0.13(4)
5	0.943	−0.07(4)	0.04(4)	0.09(6)	−0.42(6)	0.13(2)
10	0.909	−0.07(5)	0.09(6)	−0.29(6)	−0.17(6)	0.06(2)
15	0.867	0.02(6)	−0.10(7)	−0.18(6)	−1.06(6)	0.10(2)
20	0.813	−0.50(7)	0.01(8)	−2.03(6)	−0.04(6)	0.16(2)
25	0.739	0.50(9)	0.6(1)	2.41(6)	0.53(6)	−0.72(2)
30	0.466	0.40(1)	0.5(1)	−1.04(6)	2.93(6)	0.56(4)

parameter is shown as a function of γ in Fig. 10(c). A power-law fit yielded the parameters $S(0)=0.961(4)$, $\gamma_c=29.6(1)°$, and $\alpha=0.143(4)$; the fit is shown in Fig. 10(c).

Equations (8) and (9) were evaluated using the results from immense N-V-T MC simulations. In general we carried out runs consisting of $\sim 4 \times 10^6$ attempted MC translations and rotations per molecule. In all cases the components of **P** fluctuated about zero, but long runs were required to ensure that the average polarization $\langle\mathbf{P}\rangle$ was almost zero. Results for the reduced flexoelectric coefficients $e_1^*=e_1\sigma^2/\mu$ and $e_3^* = e_3\sigma^2/\mu$ in the CSSM and CLJM systems are presented in Table II and Fig. 10. Also included in Table II are the components of the average polarization $\langle\mathbf{P}\rangle$ and estimated uncertainties. In both the CSSM and CLJM systems, the measured flexoelectric coefficients are small when the molecular bend angles are less than about 20°. For more pronounced bend angles, both the splay and the bend coefficients deviate significantly from zero. The results for e_3^* are encouraging, but there is some concern over the measured values of e_1^*; naively we would expect that the splay coefficients should be small for banana-shaped molecules with transverse dipoles. Table II yields a valuable clue: The measured flexoelectric coefficients deviate significantly from zero in those simulations where there is a more pronounced average polarization. Therefore, it may be that the simulations are still not long enough to ensure a reliable evaluation of the fluctuation formulas. It is perhaps worth pointing out that during the course of the atomistic simulations performed by Cheung *et al.* there was a "small net polarization:"[35] The magnitudes of the average polarizations ($P \sim 10^{-28}$ C m^{-1}) and the average molecular dipole moments ($\mu \sim 10^{-29}$ C m^{-1}) give reduced polarizations $P/\mu \sim 10$, which are large compared with the average polarizations reported in Table II. It is possible that neither the estimates of Cheung *et al.* nor the current estimates are particularly reliable. We attempted to make *ad hoc* corrections to the fluctuation formulas in Eqs. (8) and (9) by

evaluating terms such as $\langle(P_\alpha - \langle P_\alpha\rangle)(\Pi_{\beta\gamma} - \langle\Pi_{\beta\gamma}\rangle)\rangle$, but these resulted in insignificant changes to the values of e_1 and e_3.

Notwithstanding the potential problems highlighted above, we can attempt to make some useful comments on the measured values of e_3. At the highest bend angles, $\gamma = 20° - 30°$, the magnitude of the reduced bend flexoelectric coefficient is in the region of 0.5. With typical values of $\sigma \sim 0.5$ nm and $\mu \sim 1$ D, this reduced value corresponds to a real bend flexoelectric coefficient of $e_3 \sim 7$ pC m^{-1}. This is in good agreement with typical values of $e_3 \sim 10$ pC m^{-1} measured in experiments.[29,30] It is therefore reasonable to suggest that the steric or packing contributions to the flexoelectric effect are significant. The roles of dipolar and quadrupolar electrostatic interactions must surely be at least as significant, and these should be studied in a systematic fashion. For now, though, we conclude that short-range interactions between bent-core molecules are as important in giving rise to flexoelectricity as they are in dictating the short-range structure of dense atomic liquids.[46] In drawing this analogy perhaps we should not be too surprised by the current observations. The reduced densities of spheres in the CSSM and CLJM systems are equal to $7\rho^* \sim 0.7$ at which packing effects and short-range correlations are particularly pronounced (recall that the triple-point density for the Lennard-Jones system is in the region of 0.85).

IV. CONCLUSIONS

In this work the structure, phase behavior, and flexoelectricity of model bent-core molecules have been studied using MC computer simulations. The molecular bent core consists of a "V"-shaped rigid array of soft spheres, with a transverse point dipole moment aligned along the C_2 symmetry axis.

In a linear seven-sphere nonpolar model, isotropic, nematic, smectic A, and tilted smectic F (herringbone) phases are

observed. With an opening angle of 160° the smectic A is absent, while an opening angle of 140° gives rise to a direct tilted smectic F–isotropic transition. The effects of dipolar interactions were seen to depend on the opening angle. In the linear-molecule systems these interactions appeared to destabilize the nematic and smectic A phases. In the bent-core systems, dipolar interactions reduced the degree of molecular tilt in the tilted smectic phases; this is a significant observation, particularly since dipolar interactions have often been cited as the cause of spontaneous chiral symmetry breaking in some bent-core liquid crystals.[4] Chirality arises in this case from the correlation between the molecular tilt within smectic layers and the long-range ordering of smectic-layer polarizations. Although spontaneous (anti)ferroelectric order will be favored by long-range dipolar interactions, the observation that these same interactions reduce molecular tilt seems to suggest that there may be another explanation for chirality in banana liquid crystals.[5–7]

Real bent-core liquid crystals often possess flexible tail groups at the ends of the rigid bent core, and so CBMC simulations of a flexible-rigid-flexible model were performed. Each molecule consisted of a five-sphere rigid bent core and a three-segment flexible tail attached to each end. We could only find smectic and isotropic phases, but significantly the smectic phases showed no spontaneous tilt. This is probably due to the tails providing a lubricating barrier between the smectic layers that serves to decorrelate the order within neighboring layers. Hence, the addition of molecular flexibility is likely to mitigate against the type of entropic "sawtooth" mechanisms that have been found to stabilize antiferroelectric ordering in hard-particle bent-core models.[6] The addition of the flexible tails was also seen to give rise to significant spatial fluctuations in the smectic layers. It is worth pointing out that the smectic phases of rigid model molecules are often far more ordered than real smectics (as evidenced by scattering experiments[28]). The introduction of molecular flexibility therefore brings the model systems in to better correspondence with experiment.

Finally, the flexoelectric properties of nonpolar seven-sphere bent-core molecules—with and without attractive interactions—have been studied by calculating the splay and bend coefficients in the nematic phase using fluctuation relations derived from linear-response theory.[44,45] An immense investment of computational effort was required to obtain reasonable results via this route, which serves to highlight how careful one must be in evaluating the required formulas. Nonetheless, our results show that a significant flexoelectric response can be measured for opening angles below about 150°. With typical molecular dimensions and dipole moments, the measured flexoelectric coefficients are in the region of 10 pC m^{-1} which is in excellent agreement with experiment. The flexoelectric response of real bent-core liquid crystals is often attributed largely to dipolar and quadrupolar interactions, but our results show that the molecular shape is also significant. This should not be too much of a surprise, since most thermotropic nematics are, after all, dense molecular liquids, and it is well known that the structure and dynamics in such systems are dictated by short-range repulsive interactions. We are in no way suggesting that electro-

static interactions are insignificant, and we have not studied flexoelectricity in dipolar or quadrupolar systems because of the computational effort which will probably be required to obtain reliable results. A systematic study of this point is required, and will hopefully be the subject of future papers.

[1] T. Niori, T. Sekine, J. Watanabe, T. Furukawa, and H. Takezoe, J. Mater. Chem. **7**, 1231 (1996).
[2] R. Macdonald, F. Kentischer, P. Warnick, and G. Heppke, Phys. Rev. Lett. **81**, 4408 (1998).
[3] A. Jákli, S. Rauch, D. Lötzsch, and G. Heppke, Phys. Rev. E **57**, 6737 (1998).
[4] N. V. Madhusudana, Mol. Cryst. Liq. Cryst. **409**, 371 (2004).
[5] A. V. Emelyanenko and M. A. Osipov, Phys. Rev. E **70**, 021704 (2004).
[6] Y. Lansac, P. K. Maiti, N. A. Clark, and M. A. Glaser, Phys. Rev. E **67**, 011703 (2003).
[7] D. J. Earl, M. A. Osiopov, H. Takezoe, Y. Takanishi, and M. R. Wilson, Phys. Rev. E **71**, 021706 (2005).
[8] P. J. Camp, M. P. Allen, and A. J. Masters, J. Chem. Phys. **111**, 9871 (1999).
[9] R. Memmer, Liq. Cryst. **29**, 483 (2000).
[10] S. J. Johnston, R. J. Low, and M. P. Neal, Phys. Rev. E **65**, 051706 (2002).
[11] S. J. Johnston, R. J. Low, and M. P. Neal, Phys. Rev. E **66**, 061702 (2002).
[12] J. Xu, R. L. B. Selinger, J. V. Selinger, and R. Shashidhar, J. Chem. Phys. **115**, 4333 (2001).
[13] A. Dewar and P. J. Camp, Phys. Rev. E **70**, 011704 (2004).
[14] S. C. McGrother, A. Gil-Villegas, and G. Jackson, J. Phys.: Condens. Matter **8**, 9649 (1996).
[15] S. C. McGrother, A. Gil-Villegas, and G. Jackson, Mol. Phys. **95**, 657 (1998).
[16] A. Gil-Villegas, S. C. McGrother, and G. Jackson, Chem. Phys. Lett. **269**, 441 (1997).
[17] K. Satoh, S. Mita, and S. Kondo, Chem. Phys. Lett. **255**, 99 (1996).
[18] R. Berardi, S. Orlandi, and C. Zannoni, Chem. Phys. Lett. **261**, 357 (1996).
[19] E. Gwozdz, A. Brodka, and K. Pasterny, Chem. Phys. Lett. **267**, 557 (1997).
[20] J. S. van Duijneveldt and M. P. Allen, Mol. Phys. **92**, 855 (1997).
[21] C. McBride, C. Vega, and L. G. MacDowell, Phys. Rev. E **64**, 011703 (2001).
[22] C. McBride and C. Vega, J. Chem. Phys. **117**, 10370 (2002).
[23] M. R. Wilson, J. Chem. Phys. **107**, 8654 (1997).
[24] F. Affrouard, M. Kroger, and S. Hess, Phys. Rev. E **54**, 5178 (1996).
[25] J. S. van Duijneveldt, A. Gil-Villegas, G. Jackson, and M. P. Allen, J. Chem. Phys. **112**, 9092 (2000).
[26] H. Fukunaga, J.-I. Takimoto, and M. Doi, J. Chem. Phys. **120**, 7792 (2004).
[27] R. B. Meyer, Phys. Rev. Lett. **22**, 918 (1969).
[28] P. G. de Gennes and J. Prost, *The Physics of Liquid Crystals*, 2nd ed. (Clarendon, Oxford, 1993).
[29] P. R. M. Murthy, V. A. Raghunathan, and N. V. Madhusudana, Liq. Cryst. **14**, 483 (1993).
[30] A. G. Petrov, in *Physical Properties of Liquid Crystals: Nematics*, edited by D. A. Dunmur, A. Fukuda, and G. R. Luckhurst (The Institute of Electrical Engineers, London, 2001), p. 251.
[31] J. Stelzer, R. Berardi, and C. Zannoni, Chem. Phys. Lett. **299**, 9 (1998).
[32] J. L. Billeter and R. A. Pelcovits, Liq. Cryst. **27**, 1151 (2000).
[33] A. V. Zakharov and R. Y. Dong, Eur. Phys. J. E **6**, 3 (2001).
[34] A. V. Zakharov and A. A. Vukulenko, Crystallogr. Rep. **48**, 738 (2002).
[35] D. L. Cheung, S. J. Clark, and M. R. Wilson, J. Chem. Phys. **121**, 9131 (2004).

[36] M. P. Allen and D. J. Tildesley, *Computer Simulation of Liquids* (Clarendon, Oxford, 1987).

[37] J. I. Siepmann and D. Frenkel, Mol. Phys. **75**, 59 (1991).

[38] D. Frenkel and B. Smit, *Understanding Molecular Simulation*, 2nd ed. (Academic, London, 2002).

[39] C. Zannoni, in *The Molecular Physics of Liquid Crystals*, edited by G. R. Luckhurst and G. W. Gray (Academic, New York, 1979), pp. 191–220.

[40] G. W. Gray and J. W. G. Goodby, *Smectic Liquid Crystals: Textures and Structures* (Leonard Hill, London, 1984).

[41] I. M. Withers, C. M. Care, and D. J. Cleaver, J. Chem. Phys. **113**, 5078 (2000).

[42] G. V. Paolini, G. Ciccotti, and M. Ferrario, Mol. Phys. **80**, 297 (1993).

[43] A. Galindo, C. Vega, E. Sanz, L. G. MacDowell, E. de Miguel, and F. J. Blas, J. Chem. Phys. **120**, 3957 (2003).

[44] V. B. Nemtsov and M. A. Osipov, Sov. Phys. Crystallogr. **31**, 125 (1986).

[45] M. P. Allen and A. J. Masters, J. Mater. Chem. **11**, 2678 (2001).

[46] J.-P. Hansen and I. R. McDonald, *Theory of Simple Liquids* (Academic, London, 1986).